Quantum Electronics **49** (12) 1121 – 1126 (2019)

https://doi.org/10.1070/QEL17165

Coherent optical frequency-domain reflectometer based on a fibre laser with frequency self-scanning

A.Yu. Tkachenko, I.A. Lobach, S.I. Kablukov

Abstract. **The first results of an experimental study of a coherent optical frequency-domain reflectometer (C-OFDR) based on a simple single-frequency fibre laser with frequency self-scanning are presented. The self-scanning laser generates microsecond pulses, and its lasing frequency changes linearly with a change in the pulse number without using any actively tuned elements. In addition, the generation of each pulse occurs on only one longitudinal mode with a linewidth less than 1 MHz. This laser is characterised by a high linearity of frequency tuning, due to which reflectograms can be measured without any additional spectral correction. The C-OFDR demonstrates a possibility of attaining a spatial sampling of ~200 μm and a reflectance sensitivity of approximately down to –80 dB at a test line length of ~9 m.**

Keywords: *coherent optical frequency-domain reflectometer, self-scanning fibre laser, tunable laser, fibre sensor, reflectometry.*

1. Introduction

Optical reflectometry is a key technology for both diagnostics of optical systems and distributed sensor measurements. In the latter case one uses the dependence of the parameters (e.g., intensity or optical frequency) of the radiation scattered along an optical fibre on external physical impacts (for example, temperature or mechanical strain) [1]. Time-domain reflectometry is most often used in distributed fibre sensor systems. The reflectometer operation is based on probing a fibre line with short radiation pulses. The probe radiation, reflected from defects or scattered from fibre refractive index inhomogeneities (Rayleigh scattering), is detected and analysed according to the echo principle, in correspondence with which the reflector/scatterer position is linearly related to the delay time between the input and reflected signals. In this case the reflectometer spatial resolution is determined by the pulse duration and may reach ~1 m.

However, some applications (for example, airplane construction monitoring) call for a much better spatial resolution. The simplest way to improve resolution is to reduce the probe pulse duration, which leads (provided that the peak power is preserved) to a decrease in the signal-to-noise ratio and, as a consequence, reduces the reflectometer sensitivity to measured power. To solve this problem, it is necessary to increase the probe-pulse peak power. However, it is limited by the nonlinear processes occurring in the fibre (for example, stimulated Raman scattering) [2], which distort the measured signal. Another approach to reducing the noise level is to apply single-photon counters. For example, using a single-photon counter, Legré et al. [3] obtained a spatial resolution on the order of several centimetres for a 50-km-long line. Special methods of backscattered signal processing are also applied to improve spatial resolution. The coding/decoding technique using codes of different types [4, 5] (for example, simplex-coding) allows one to increase the signal-to-noise ratio without changing the pulse duration. In this case, the probe signal is a coded sequence of standard pulses. Or, in contrast, the coding technique makes it possible to reduce the spatial resolution with preserving the signal-to-noise ratio. The signal deconvolution technique, which takes into account the pulse shape, also improves spatial resolution [6].

A radically different approach to increasing spatial resolution is the application of coherent optical frequency-domain reflectometry (for brevity, optical frequency-domain reflectometry) [7]. Its operation principle differs from the echo principle and is based on spectral analysis of the interference signal arising when probe and scattered beams are mixed. In this case, the spatial coordinate of reflectors/scatterers is proportional to the frequency coordinate of maxima in the Fourier spectrum of the interference signal measured during optical frequency tuning. Tunable radiation sources with a large coherence length are used for coherent optical frequency-domain reflectometers (C-OFDRs). The C-OFDR spatial resolution is limited by the tuning range of probe laser wavelength. Lasers of different types have been applied as probe ones. Examples are a current-tuned semiconductor laser [8] and a Nd : YAG ring laser tuned by varying temperature [9] or using piezoelectric transducers [10]. A drawback of these sources is their small coherence length and frequency tuning nonlinearity. Fourier transform signal processing calls for strict linearity of optical frequency tuning. Generally a trigger interferometer is used to compensate for tuning nonlinearity [11]. In essence, the interferometer is necessary for measuring the instantaneous optical frequency. As a result, one can obtain reflection signals with a periodicity determined by regular frequency tuning intervals.

The drawbacks related to the limited coherence length and tuning nonlinearity can be eliminated using a laser diode

A.Yu. Tkachenko Institute of Automation and Electrometry, Siberian Branch, Russian Academy of Sciences, prosp. Akad. Koptyuga 1, 630090 Novosibirsk, Russia; e-mail: alinka.tkacenko@yandex.ru;
I.A. Lobach, S.I. Kablukov Institute of Automation and Electrometry, Siberian Branch, Russian Academy of Sciences, prosp. Akad. Koptyuga 1, 630090 Novosibirsk, Russia; Novosibirsk State University, ul. Pirogova 2, 630090 Novosibirsk, Russia

Received 21 October 2019
Kvantovaya Elektronika **49** (12) 1121 – 1126 (2019)
Translated by Yu.P. Sin'kov

with an external cavity based on a fibre Bragg grating [12]. This scheme made it possible to obtain linear frequency tuning in a range of 200 MHz with a linewidth of 10 kHz. As a result, the spatial resolution in this system was improved to 2 m at a line length of 115 m. The spatial resolution of commercially available C-OFDRs is already 20 μm on a 20-m-long fibre line [13]. A higher spatial resolution was demonstrated on experimental samples. In the case of widely tunable laser sources, further improvement of resolution is limited by the dispersion characteristics of the tested medium. A spatial resolution of ~5 μm was demonstrated in experiments with waveguides based on an InP crystal in [14], where the dispersion waveguide characteristics were taken into account. The maximum length of measured line for the C-OFDR is generally limited by the source coherence length. The method of compensating for phase noise [15] allows one to increase the line length up to 10 km; however, the maximum line length in real devices is limited by the probe radiation frequency sampling.

In this study we propose to use a new type of a tunable laser with frequency self-scanning [16] as a probe radiation source to implement strict discreteness during frequency tuning. Optical frequency tuning occurs due to the internal processes occurring in the active fibre [16], without using any tunable elements. An important feature of this laser is the generation of a sequence of microsecond coherent pulses with a spectral width no more than 1 MHz and strict discreteness of optical frequency. Due to the latter circumstance, this laser can be used without any trigger interferometer for compensating the frequency tuning nonlinearity.

2. Experimental

A schematic diagram of the C-OFDR is shown in Fig. 1. A key element of the scheme is a fibre laser with frequency self-scanning. Polarisation-maintaining components and fibres are used in the laser design. The laser cavity is formed by a broadband highly reflective fibre loop mirror based on a 50/50 polarising coupler and a right angle cleaved fibre end with Fresnel reflection. A 3-m-long double-cladding Nufrn PM-YDF-5/130 fibre, doped with ytterbium ions, was used as a gain medium. The latter was pumped through a pump combiner by a multimode laser diode with a wavelength close to 975 nm and a power up to 9 W. The 80% port of the 20/80 coupler serves (spliced with an isolator) for extraction of laser radiation from the cavity and its further use. As a result, the effective reflectance of the output mirror in the form of the cleaved fibre end was ~0.2%. Then 10% of all output radiation power was transmitted through a 10/90 coupler to form a reference channel. At a pump power of 2 W the laser operates in the mode of wavelength self-scanning in the range of 1060–1080 nm with a rate of ~1 nm s^{-1} (see Fig. 1). The laser intensity dynamics (similar to the dynamics considered in [16]) is a set of intensities of periodic microsecond single-frequency pulses (Fig. 2a) with a spectral width no more than ~1 MHz. Note that this is an estimate rather than the exact linewidth value, because it is related to the small variation in the optical frequency during one-pulse generation time (it describes the so-called frequency chirp) and is made using the heterodyning technique. The real instantaneous linewidth is expected to be smaller than the frequency chirp. Even in this case the laser radiation coherence length can be estimated as approximately 200 m. The lasing frequency changes between pulses by a value of one laser cavity mode spacing and amounts to ~5.5 MHz.

The 25-mW radiation of the laser with frequency self-scanning is transmitted through a Mach–Zehnder interferometer, one of whose arms contains a line under test (LUT) (the inner rectangle on the right-hand side of the schematic in Fig. 1). Note that, since the entire scheme was implemented on polarisation-maintaining fibres and components, we did not have to tune additionally polarisation states of signals, as was necessary to do in [12]. The interferometer consists of three fibre couplers, which form reference and measurement channels. The first coupler (99/1) divides the laser beam between the measurement and reference channels in the corresponding proportion. A piece of passive 4-m-long fibre was introduced into the reference channel to equalise the optical lengths of the two arms, because the beginning of the tested line corresponded to the point providing a reflection at which the interferometer arm lengths turn out to be equal. A system consisting of a fibre attenuator and a piece of fibre with a

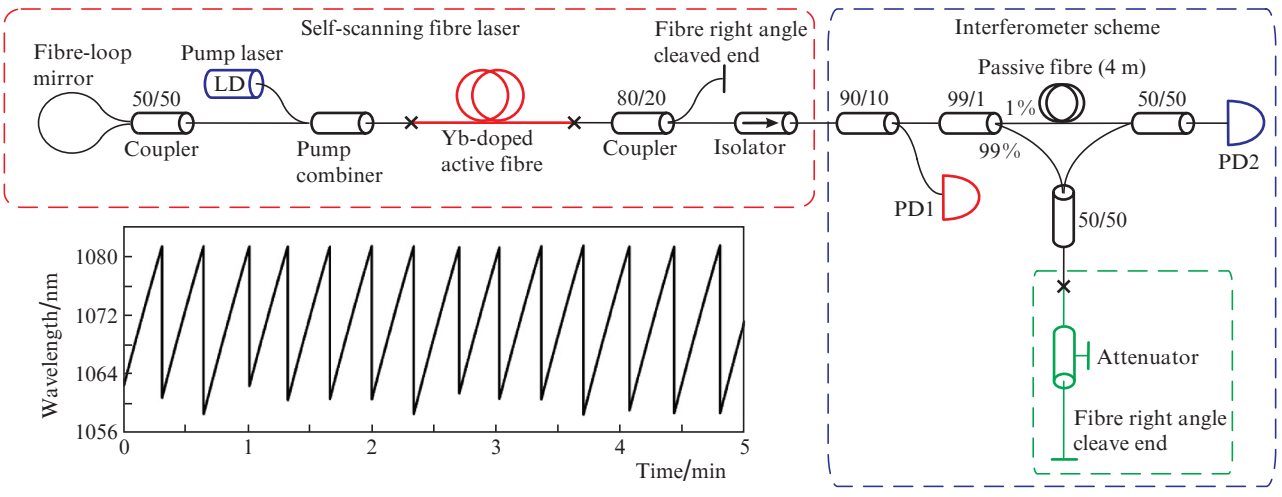

Figure 1. Schematic of a C-OFDR based on a fibre laser with frequency self-scanning. The characteristic lasing spectrum dynamics is shown in the inset.

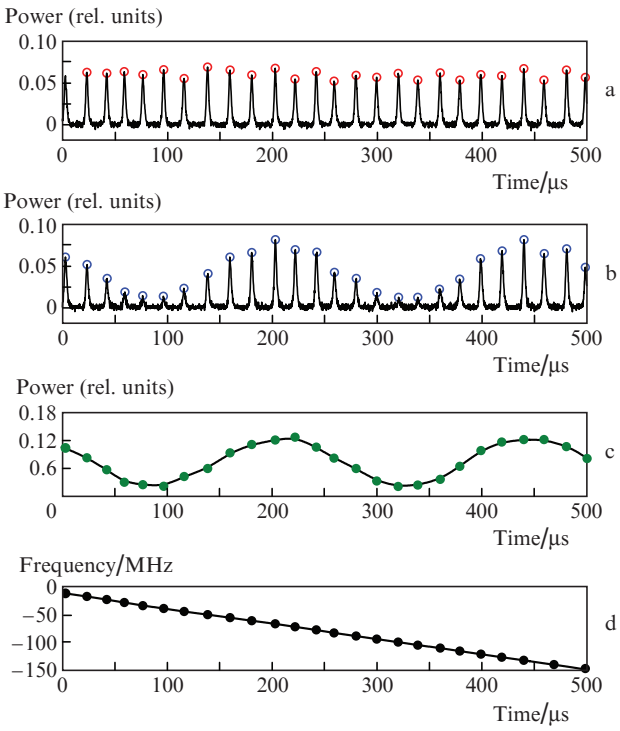

Figure 2. (a, b) Dynamics of laser pulse intensity at the (a) input and (b) output of reflectometer; (c) envelope of the interference signal, obtained from pulse-by-pulse division of the (b) output and (a) input signals; and (d) the characteristic dynamics of decreasing the laser optical frequency.

length varied during experiments served a tested fibre line. At the free side, this fibre was cleaved at a right angle to provide Fresnel reflection. The reflector position and effective reflectance value were varied by changing, respectively, the fibre length and the degree of attenuation. To monitor the degree of attenuation, we measured additionally the total power from the side of the tested-line free end. The signals at the interferometer input and output were recorded by two fast photodetectors (PD1 and PD2, respectively, in Fig. 1) with a bandwidth of 1 GHz (Thorlabs, DET01CFC) and digitised using an oscilloscope (LeCroy, WavePro 725Zi-A) in a 2-s time window with a sampling rate of 5 MHz. At this sampling rate, 30 points were recorded for a time equal to the duration of each pulse, which made it possible to reconstruct the pulse shape.

The radiation transmitted through the interferometer is a sequence of pulses with varying amplitudes, which depend on the interference result and change when the optical laser frequency is tuned. The period and magnitude of amplitude modulation contain information about the position of the reflectors in the LUT and the radiation intensity reflected by them, respectively. When there is only one reflector at the end of LUT, the envelope takes the form of a harmonic function (Fig. 2b). To eliminate the influence of input radiation power fluctuations, we performed pulse-by-pulse normalisation of the output interference signal to the reference input signal. During normalisation we sought for the peak values for each pulse in the reference signal and then calculated the ratio of the total powers in the interference and reference signals for these instants using seven nearest points (circles in Figs 2a and 2b for the reference and interference signals, respectively). In essence, we calculated the energy of each pulse, and then the pulse energy in the interference signal was normalised to the corresponding pulse energy in the reference signal (Fig. 2c). For the self-scanning laser in use, one pulse in the time domain corresponds to one certain optical frequency in the spectral region. All pulses are equidistant in the frequency domain, because the optical frequency changes from pulse to pulse by one mode beat interval $\delta\nu \approx 5.5$ MHz (Fig. 2d). As a result of the above procedure, a dependence of the normalised amplitude of interference signal on the relative pulse number i was plotted. The relative frequency was recovered by simple multiplication of the pulse number by the frequency mode spacing: $\nu = \delta\nu i$. To obtain a reflectogram (longitudinal distribution of reflectors along the line under study), we applied a fast Fourier transform to the dependence of the normalised interference signal on the relative frequency ν. In this case, the physical meaning of the abscissa axis corresponds to the time delay between the signals in the reference and measurement channels. A transition from time to LUT coordinates is implemented by simple multiplication of time by the signal propagation velocity in the fibre. The maximum line length in these systems is limited by the value of sample rate between neighbouring pulses. This limitation is a manifestation of the sampling effect, when the digitisation step exceeds the modulation frequency of digitised signal that increases with an increase in the difference between the interferometer arm lengths. The maximum line length is estimated to be $L_{max} = c/(2n\delta\nu) = 8.7$ m, where n is the fibre refractive index and c is the speed of light.

In the first experiment we measured reflectograms at different degrees of the attenuator inserted in the tested line. Figure 3 shows examples of reflectograms for three attenuator degrees; they were obtained at average powers of 25 mW, 530 μW, and 70 μW at the output of the LUT free end.

All reflectograms contain a strong peak, corresponding to the reflection from the free output fibre end. The peak amplitude decreases with an increase in the attenuator loss. In the

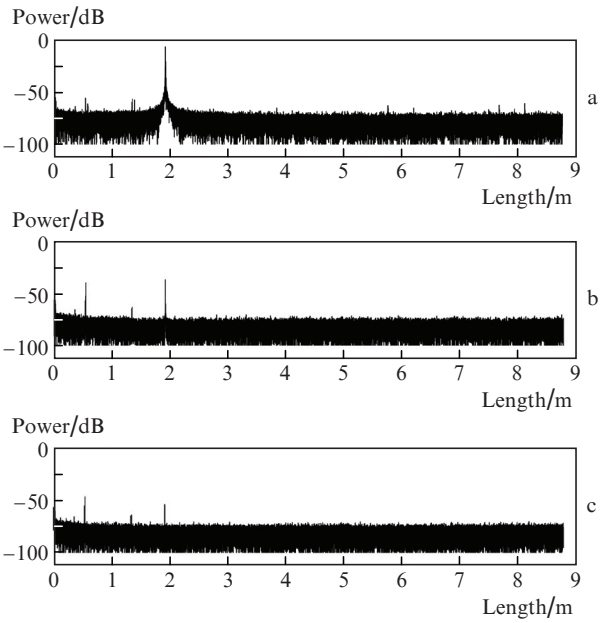

Figure 3. Reflectograms of a 1.92-m-long LUT for different degrees of single pass attenuation in the attenuator: (a) 0, (b) −16.7, and (c) −25.5 dB.

case of completely closed attenuator (i.e., when the loss is maximum) the peak due to the fibre cleaved end reflection is not observed, because it is obscured by noise. The effective reflectance from the right angle fibre cleave end can be estimated with allowance for the loss in the attenuator by measuring the radiation intensity from the LUT free end. The powers of the transmitted and reflected beams are estimated to be $P_{trans} = P_0 a\,(1-R)$ and $P_{ref} = P_0 a^2 R$, respectively, where P_0 is the power at the LUT input, a is the attenuator loss, and R is the reflectance of the output fibre end face. Thus, the effective reflectance depends quadratically on the radiation power measured from the side of the LUT free end:

$$R_{eff} = a^2 R = \frac{R P_{trans}^2}{[(1-R)P_0]^2}. \quad (1)$$

The dependence of the amplitude of the Fourier expansion component corresponding to the reflection from the output LUT end face on the effective reflectivity $10\lg R_{eff}$, found by measurement of the output power and further calculation based on expression (1), is shown in Fig. 4. Its approximation is a linear dependence with a unit slope. The intersection of the linear approximation with the noise level yields an estimate for the minimum value of measured LUT reflectivity: approximately –79 dB.

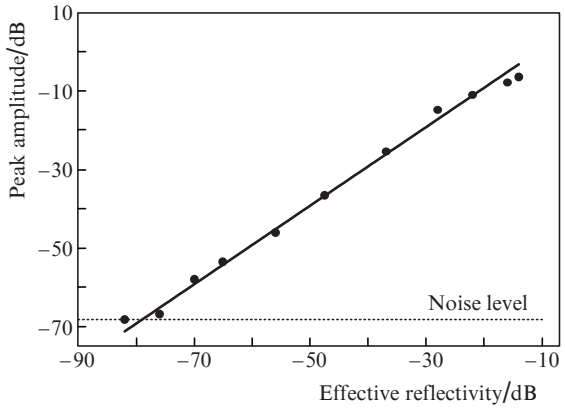

Figure 4. Dependence of the peak amplitude (peak at 1.92 m in Fig. 3) on the effective LUT reflectivity calculated from formula (1).

In the next series of experiments we measured reflectograms for the attenuator in open state (0 dB at 25 mW at the LUT output) and at different fibre lengths in the tested line. Figure 5 shows the corresponding reflectograms for LUT lengths of 3.6, 7.1, and 9.8 m.

3. Results and discussion

The reflectograms presented in Figs 3 and 5 contain, along with the main peak due to the reflection from the output LUT end face, many minor peaks. A detailed analysis of the measured reflectograms makes it possible to classify them. For convenience of description, we will divide peaks into three groups: A, B, and C. The peaks of group A are due to the reflection from the output end face, but only the position of the main peak A1 corresponds to the LUT length. More specifically, its position is consistent with the relative difference

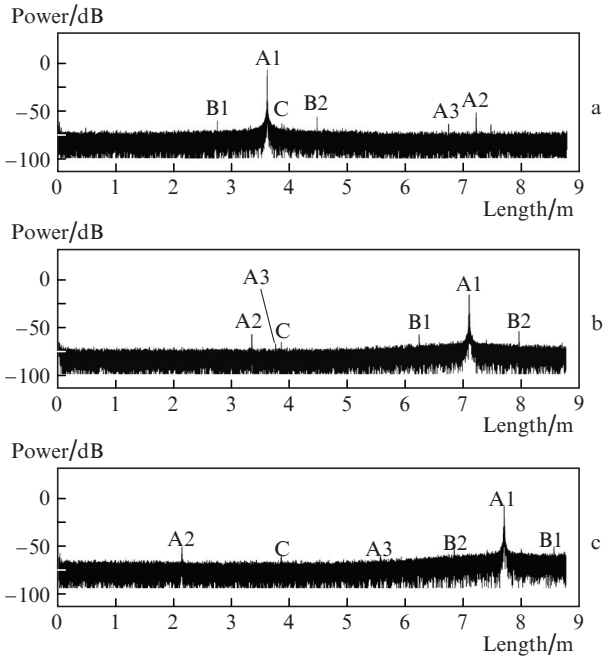

Figure 5. Reflectograms of LUTs with lengths of (a) 3.6, (b) 7.1, and (c) 9.8 m with an open attenuator.

in the interferometer arm lengths; therefore, the interferometer arms were equalised without test line in the initial stage of experiments. Let us illustrate the reflectometer operation by the case where the LUT length exceeds the maximum operation length of the reflectometer (determined by the frequency discretisation step), L_{max} = 8.7 m (Fig. 5c). In this case the position of peak A1 in the reflectogram (L_{meas} = 7.6 m) is inconsistent with the real reflector position (L_{real} = 9.8 m). This corresponds to the situation where the signal digitisation rate is lower than the measured modulation frequency. For small excesses of real measured length above the L_{max} value ($L_{max} < L_{real} < 2L_{max}$), in correspondence with the properties of the fast Fourier transform, the position in the reflectogram is given by the expression

$$L_{meas} = 2L_{max} - L_{real}. \quad (2)$$

The positions of the other two peaks of group A (A2 and A3), which have a smaller amplitude in Fig. 5, can be assigned to higher (second and third) harmonics of main peak A1. In most cases the positions of these peaks go beyond the maximal measurement length, and then the peak abscissas in the reflectogram are determined by expression (2). These signals indicate that the interference signal differs from a pure harmonic function, which is valid for the Mach–Zehnder interferometer. A possible reason for this difference is that the photodetector sensitivity is somewhat nonlinear, which manifests itself when measuring amplitudes of signals.

Along with these signals, the reflectogram contains spurious peaks, which are not related to any real beam reflections in the LUT. Note also that the amplitude of spurious peaks is 30–40 dB smaller than that of the main peak A1. Two peaks of group B (peaks B1 and B2) are spaced symmetrically by 0.86 m from the main reflection peak. These peaks can be

related to the frequency modulation of the initial laser signal. A peak at a length of 0.86 m was also observed in the Fourier spectrum of the reference signal. One might suggest that the laser cavity contains a spurious embedded interferometer, whose origin was not revealed. Group C contains one peak (at 3.85 m), whose position is independent of the experimental conditions. Since the position of peaks of this type is invariable, they can be related to regular electric interference in the measurement scheme. Note that similar spurious peaks, caused by electrical and optical signals, were also observed in reflectograms in other studies, e.g., in [12]. To provide correct operation of a frequency reflectometer, it is necessary to suppress such interfereing factors, specifically: exclude the occurrence of external electric interference in the measurement scheme, ensure photodetector operation in the linear mode, and exclude any spurious reflections both in the laser and in the measurement interferometer. According to an estimate, the level of spurious reflections should not exceed the C-OFDR sensitivity, i.e., –90 dB. In particular, we should note that standard fibre connectors APC/FC cannot provide this level of backward reflection. Special attention must be paid to the level of backward reflection of all elements in the system: couplers, isolators, and splicing points.

Note also that not all additional peaks in the reflectograms were spurious. When the attenuator had a significant degree of attenuation (see, e.g., Fig. 3c), an additional peak arose in the reflectogram, which corresponded to attenuator's position in the line (the peak at 0.54 m in Fig. 3c) with a Fourier component amplitude of $-40\ldots-50$ dB. One can relate this feature to the reflections arising in the attenuator with an increase in the loss in it. Based on the dependence presented in Fig. 4, one can estimate the reflectance from the attenuator at a level of $-50\ldots-60$ dB, which is in agreement with its certified data (–54 dB). This peak is practically absent for a completely open attenuator (Fig. 3a).

The signal spatial sampling δl turned out to be ~200 μm; this value is determined by the laser frequency tuning range $\Delta\nu$: $\delta l = c/(2n\Delta\nu)$. When signal is measured during 2 s, the tuning range $\Delta\nu$ is ~0.5 THz (which corresponds to a spatial sampling of 200 μm). The FWHM of the reflection peak in reflectograms does not exceed 300 μm, which can be considered as the spatial resolution of the implemented scheme. Note that this value can be reduced to ~20 μm using the full tuning range of the laser (~7 THz) in measurements. However, the measurement time in our experiments was limited by the size of the files digitised with a digital oscilloscope.

4. Conclusions

The first results of the experimental study of coherent optical frequency-domain reflectometer based on a fibre laser with frequency self-scanning are reported. The lasing frequency of this laser is tuned without any active tunable elements. An important feature of the scheme proposed is the absence of trigger interferometer because of the stepwise frequency tuning in the laser source. The scheme was approved on a fibre line consisting of a fibre attenuator and a fibre segment with Fresnel reflection at the free output end face. The scheme demonstrated that the reflectometer can operate with a spatial sampling of ~200 μm and a sensitivity of about down to –80 dB at a test line length of ~9 m. We can outline the following ways of improving the presented reflectometric system. Its spatial resolution can be improved up to ~15 μm using the maximum tuning range of laser wavelength (~25 nm [17]) in measurements. In addition, stabilisation of the boundaries of laser scanning range (demonstrated with the aid of fibre Bragg gratings [18]) may positively affect the scan-to-scan reproducibility of reflectograms. Note also that such systems can be adapted for operation in other spectral ranges, for example, in the vicinities of 1.46 μm [19] and 1.92 μm [20] (using bismuth- and thulium-doped fibre lasers, respectively). The maximum length of measured line can be increased by reducing the frequency step for self-scanning laser. For example, a decrease in the frequency step between pulses to ~1 MHz with an increase in the active medium length (with the total cavity length equal to ~100 m) was demonstrated in [19] for a bismuth fibre laser. One might expect the maximum line length to increase to ~50 m in this case. The sensitivity of the system to backward reflection can be improved by reducing the noise level during measurements and improving the data processing algorithm (pulse-by-pulse division of interference and reference signals). Thus, the characteristics of the proposed C-OFDR scheme based on fibre laser with frequency self-scanning are expected to correspond to those of known commercial samples. At the same time, the scheme would remain simple because of the absence of tunable elements and devices for laser frequency correction.

Acknowledgements. The experimental study of A.Yu. Tkachenko was supported by the Russian Foundation for Basic Research (Grant No. 18-32-00563). The study was performed within a government contract with the IA&E SB RAS (No. 0254-2019-0001) using equipment of the Multiple-Access Centre 'High-Resolution Spectroscopy of Gases and Condensed Matter' of the IA&E SB RAS (Novosibirsk).

References

1. Hartog A.H. *An Introduction to Distributed Optical Fibre Sensors* (Boca Raton, USA: CRC Press, 2018) p. 442.
2. Agrawal G. *Nonlinear Fiber Optics* (Cambridge, USA: Academic Press, 2012).
3. Legré M., Thew R., Zbinden H., Gisin N. *Opt. Express*, **15**, 8237 (2007).
4. Jones M.D. *IEEE Photon. Technol. Lett*., **5**, 822 (1993).
5. Lee D., Yoon H., Kim P., Park J., Kim N.Y., Park N. *IEEE Photon. Technol. Lett*., **17**, 163 (2005).
6. Bahrampour A.R., Maasoumi F. *Opt. Fiber Technol*., **16**, 240 (2010).
7. MacDonald R.I. *Appl. Opt*., **20**, 1840 (1981).
8. Uttam D., Culshaw B. *J. Lightwave Technol*., **3**, 971 (1985).
9. Sorin W.V., Donald D.K., Newton S.A., Nazarathy M. *IEEE Photon. Technol. Lett*., **2**, 902 (1990).
10. Venkatesh S., Sorin W.V., Donald D.K., Heffner B.L. *Coherent FMCW Reflectometry Using a Piezoelectrically Tuned Nd:YAG Ring Laser in 8th Optical Fiber Sensors Conference* (Monterey, CA, USA, 1992).
11. Huang K., Carter G.M. *IEEE Photon. Technol. Lett*., **6**, 1466 (1994).
12. Soller B.J., Gifford D.K., Wolfe M.S., Froggatt M.E. *Opt. Express*, **13**, 666 (2005).
13. https://lunainc.com.
14. Zhao D., Pustakhod D., Williams K., Leijtens X. *IEEE Photon. Technol. Lett*., **29**, 1379 (2017).
15. Ito F., Fan X., Koshikiya Y. *J. Lightwave Technol*., **30**, 1015 (2012).

16. Lobach I.A., Kablukov S.I., Podivilov E.V., Babin S.A. *Laser Phys. Lett*., **11**, 045103 (2014).
17. Lobach I.A., Tkachenko A.Yu., Kablukov S.I. *Laser Phys. Lett*., **13**, 045104 (2016).
18. Tkachenko A.Yu., Lobach I.A., Podivilov E.V., Kablukov S.I. *Quantum Electron*., **48**, 1132 (2018) [*Kvantovaya Elektron*., **48**, 1132 (2018)].
19. Lobach I.A., Kablukov S.I., Melkumov M.A., Khopin V.F., Babin S.A., Dianov E.M. *Opt. Express*, **23**, 24833 (2015).
20. Budarnykh A.E., Vladimirskaya A.D., Lobach I.A., Kablukov S.I. *Opt. Lett*., **43**, 5307 (2018).